Mechanical sensors

3-D Printed Graphene-Based Piezoresistive Foam Mat for Pressure Detection Through Electrical Resistance Tomography and Machine Learning Classification Techniques

Nicola Pesce[1,2], Marco Fortunato[1,2], and Alessio Tamburrano[1,2*]

[1]*Department of Astronautical, Electrical and Energy Engineering (DIAEE), Sapienza University of Rome, 00184 Rome, Italy*
[2]*Nanotechnology Research Center Applied to Engineering (CNIS), Sapienza University of Rome, 00185 Rome, Italy*
[*]*Senior Member, IEEE*

Manuscript received 26 July 2023; revised 8 August 2023; accepted 12 August 2023. Date of publication 21 August 2023; date of current version 29 August 2023.

Abstract—This letter presents the development and investigation of a novel soft piezoresistive foam mat sensor (FMS) based on graphene nanoplatelets (GNPs) for pressure sensing. The sensor is fabricated using a 3-D printed polyvinyl alcohol (PVA) water-soluble sacrificial template, which is then infiltrated with Ecoflex polymer and dip-coated in a GNP-ethanol solution. The mechanical response as well as the high piezoresistive sensitivity (0.31 kPa^{-1} @ 8 kPa) of the fabricated foam is assessed experimentally. Pressure detection is achieved through electrical resistance tomography (ERT) using the opposite current injection method, and the collected data are processed using machine learning (ML) classification techniques to localize pressure application on the FMS's surface. The experimental results demonstrate the potential of the suggested approach to effectively detect pressure across extensive surface areas, achieving an accuracy of approximately 87.5% or 83.7%, respectively, for identifying the presence of deformation resulting from a single fingertip touch or from the simultaneous touch of two fingers at separate points on different zones of the FMS.

Index Terms—Mechanical sensors, pressure sensors, 3-D printing, ecoflex, electrical resistance tomography (ERT), graphene, machine learning (ML), nanoplatelets, piezoresistive mat, polymeric foam, water soluble template.

I. INTRODUCTION

Recent advances in materials science and engineering have led to the development of innovative materials with sensing properties, taking advantage of the piezoresistive phenomenon [1]. In particular, resistive pressure sensors incorporating various nanostructures, such as graphene nanoplatelets (GNPs), graphene/nanowires, or carbon nanotubes [2], [3], [4], [5], have received considerable attention. Specifically, porous graphene-based sponges [6], [7] have shown promise for creating flexible and highly sensitive pressure sensors and additive manufacturing methods are currently being explored to control foam structure [8] to optimize performance through design.

Our letter focuses on this context, investigating the feasibility of utilizing a novel 3-D printed GNP-based piezoresistive foam mat sensor (FMS) for pressure detection, using electrical resistance tomography (ERT) and machine learning (ML) techniques.

The use of large-area pressure sensing materials and ERT holds promise in overcoming the limitations of conventional discrete multisensor configurations, such as installation, synchronization, data collection and processing, limited spatial resolution, and coverage. The combination of ERT, a noninvasive imaging technique that visualizes the spatial resistivity variations within a medium by applying electrical currents and measuring voltages at its boundaries, with sensing material has been investigated in several areas, such as healthcare [9], robotics [10], and structural health monitoring (SHM) [11]. Noteworthy works have explored the combination of ERT and nanocomposites for tactile sensing in soft materials [12], [13], even employing ML techniques to solve the inverse image reconstruction problem [14], [15]. Although these studies showcased the potential of ERT, they face limitations related to image reconstruction techniques, computational complexity, data interpretation, and the requirement of substantial training data.

Our approach combines additive manufacturing, ML methods, and GNP-based piezoresistive foam, creating a powerful synergy for efficient and versatile pressure sensing suitable for various applications and introducing several advantages. First, the adopted ML methods avoid image reconstruction need, ensuring computational efficiency, simplified data interpretation, and hence future streamlined system integration. Furthermore, 3-D printing opens the path for optimizing foams performance with customizable pore structures and versatile pressure sensing in various scenarios. In addition, utilizing GNP-based piezoresistive foam offers advantages in terms of uniform coating, cost-effectiveness, ease of processing, and nontoxicity when compared to other nanomaterials [3].

In Section II, we initially describe a new flexible and highly sensitive foam-based sensor (FS) made of Ecoflex, a biocompatible elastomer forming a 3-D porous structure, and GNPs that create the piezoresistive network on the surface of the pores. To achieve this, we used polyvinyl alcohol (PVA), a water-soluble and eco-friendly material, as the sacrificial template, specifically designed and fabricated through 3-D printing to control the foam's structure and avoid stochastic pore size distribution [6], [7]. After infiltrating GNPs, we evaluated the FS properties through morphological and electromechanical tests. Then, using the same fabrication process, we developed a piezoresistive FMS for pressure detection, investigating the feasibility of using ERT in combination with ML and a grid-like approach to localize the pressure exerted with fingertips on the mat surface.

Corresponding author: Nicola Pesce (e-mail: nicola.pesce@uniroma1.it).
Nicola Pesce and Alessio Tamburrano contributed equally to this work.
Associate Editor: R. Dahiya.
Digital Object Identifier 10.1109/LSENS.2023.3307077

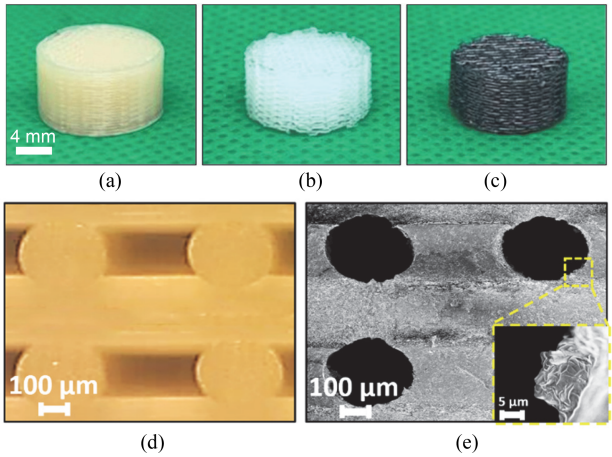

Fig. 1. (a) 3-D printed PVA sacrificial template. (b) Ecoflex open cell foam. (c) GNPs/Ecoflex foam. (d) Cross section of 3-D printed PVA template with optical microscopy. (e) FE-SEM cross section of the GNPs/Ecoflex open cell foam and a magnification of a partially embedded GNP.

II. MATERIALS AND METHODS

A. Fabrication

First, small cylindrical-shaped piezoresistive FS samples were fabricated for characterization [see Fig. 1(c)]. The samples had an average diameter of 10.5 mm ± 0.12 and thickness of 6.5 mm ± 0.10 mm. The fabrication process is briefly described as follows.

The fabrication method involved creating a porous structure that replicated the original sacrificial template [see Fig. 1(a)]. This was produced using a fused filament fabrication-based 3-D printer (Da Vinci 2.0 A Duo XYZ) equipped with two 0.4 mm nozzles. A 1.75-mm PVA filament was employed to generate the grid structure using a rectilinear infill pattern with 50% infill density and a 0.3 mm layer thickness. The resulting structure is depicted in Fig. 1(d), which was captured using an optical microscope (Nikon Eclipse LV150).

Next, a low-viscosity, skin-safe certified silicone rubber (Ecoflex 00-20, Smooth-on, Inc.) was used to infiltrate the template under vacuum (∼313 mbar) to eliminate air bubbles and ensure complete filling with the polymer. After curing at room temperature for 24 h, the samples were trimmed and immersed in water to dissolve the PVA filaments. The resulting open-cell Ecoflex foam [see Fig. 1(b)] was then dried in an oven at 60 °C for 15 min. Subsequently, it was infiltrated with a suspension of GNPs in ethanol through drop casting in a vacuum chamber to facilitate solvent evaporation. The resulting FS, with GNPs forming an electrically conductive network on the pore surface of the Ecoflex foam, exhibited piezoresistive properties. The morphology of the foam was investigated using field-emission scanning electron microscopy (FE-SEM) at an accelerating voltage of 2 kV. As shown in Fig. 1(e), the GNPs were partially embedded within the elastomer, confirming the findings of Fortunato et al. [6]. By SEM images analysis, we quantified the maximum and minimum diameters of 100 pores, yielding average values of (409 ± 21) μm and (318 ± 19) μm, respectively.

Following the illustrated process steps, a larger parallelepiped-shaped sample was fabricated to investigate the feasibility of detecting finger touches on the surface using ERT. Pictures of the produced PVA template, Ecoflex foam mat (FM), and 60 mm × 60 mm × 6.5 mm GNPs/Ecoflex FMS are reported in Fig. 2.

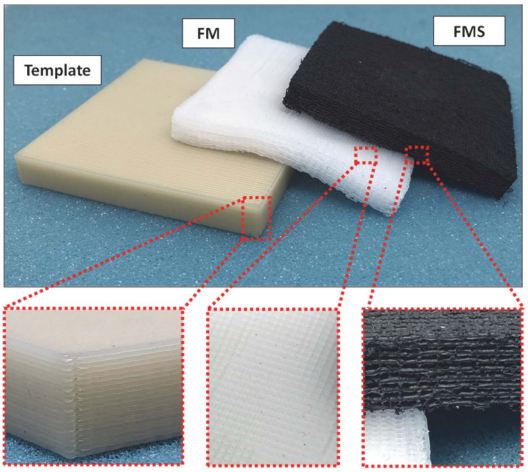

Fig. 2. 3-D printed PVA sacrificial mat template, Ecoflex FM, and GNPs/Ecoflex FMS.

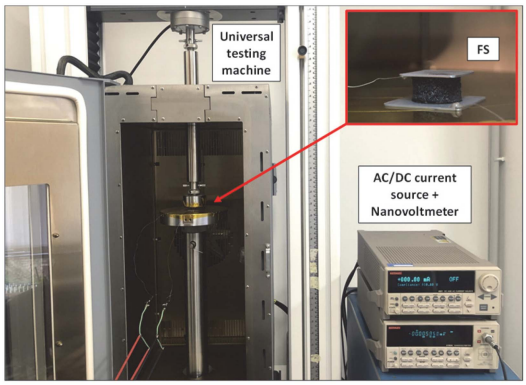

Fig. 3. Setup for compression and electromechanical tests. The inset picture shows an FS sandwiched between two aluminum parallel electrodes.

B. Mechanical and Electromechanical Characterization

The mechanical properties of the polymeric foams were investigated through quasi-static uniaxial compression tests using an Instron 3366 universal testing machine equipped with two platens and a 10 N load cell (see Fig. 3). The tests were conducted up to a maximum pressure of 30 kPa at a compression rate of 1 mm/min.

In order to investigate the piezoresistive properties, the FS sample is sandwiched between two aluminum plates, glued with a conductive epoxy resin. Tin coated copper wires (32 AWG) are then attached to the aluminum plates for electrical contact (see inset image of Fig. 3). The FS sample is subjected to a compression test while simultaneously measuring the resistance using a two-wire volt-amperometric technique. The measurements are conducted using a Keithley 6221 dc/ac current source and a Keithley 2182 nanovoltmeter. During the test, a dc current with an amplitude of 10 μA is injected into the FS sample and the resistance change is evaluated by measuring the voltage across the sample as a function of the applied load or strain.

C. Electrical Resistance Tomography

For the implementation of ERT on the FMS, we utilized an "across" injection current method known as the opposing scheme [11]. A 10 μA current is injected through two electrodes positioned on opposite sides of FMS. This process is repeated for all 16 electrodes strategically

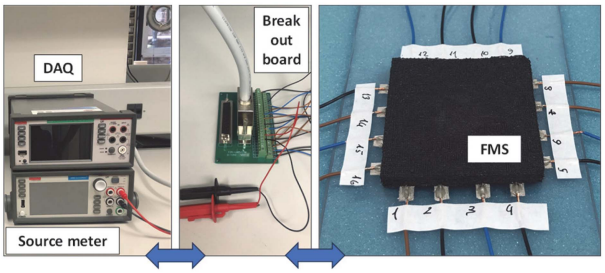

Fig. 4. Experimental setup for the ERT applied to FMS.

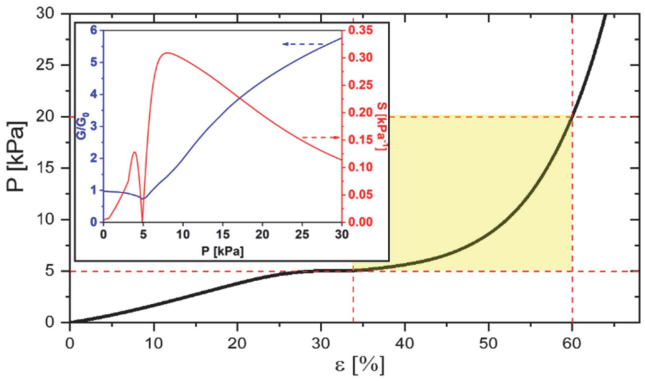

Fig. 5. Pressure–strain curve obtained with quasi-static compression test. The inset figure shows the normalized conductance and the calculated sensitivity versus pressure. The shaded area refers to the typical range of pressure exerted by a finger on the mat.

placed along the outer edge of the FMS's bottom surface. By doing so, we are able to measure the electric potential difference between pairs of opposing electrodes, including those responsible for injecting the current. This results in a total of 16 voltage measurements for each current injection, generating a dataset of 256 voltage data points (sampled at a rate of 40 Hz). The entire procedure is repeated multiple times to generate a voltage values dataset suitable for training ML algorithms. The equipment used for this setup includes a Keithley DAQ6510 with a Matrix 7709 card, a Keithley 2450 current generator, a D-sub to 50-pin serial cable, and a DSUB DB50 Male/Female Header Breakout Board connected to the FMS electrodes (see Fig. 4). Remote control of the data acquisition system is achieved through a PC with TSP programming language, enabling the management of multiplexing tasks such as current injections and voltage measurements across electrode pairs.

III. RESULTS AND DISCUSSION

A. Performance of Piezoresistive Foams

Fig. 5 illustrates the pressure (P)–strain (ε) curve obtained from the compression test of the Ecoflex foam sample. It also presents the measured variation of the conductance G normalized to its initial value at rest (G_0) and the calculated sensitivity $S = |\frac{\partial G}{\partial P}| \cdot G_0^{-1}$ of the FS sample. The P–ε curve exhibits the typical three-zone pattern observed in compressed foams: a linear elastic region (up to ~20% strain), a quasi-plateau region, and a densification region that occurs at strains exceeding 30%. This behavior has an impact on the foam's conductivity and sensitivity. The sample shows both negative and positive piezoresistive responses across the tested pressure range,

TABLE 1. Accuracy of the Various ML Algorithms

Models	Accuracy (only ST)	Accuracy (ST & DT)
SVM	*87.5%*	*81.4%*
ANN	*79.2%*	*72.7%*
KNN	*83.3%*	*83.7%*
Decision tree	*45.8%*	*52.3%*

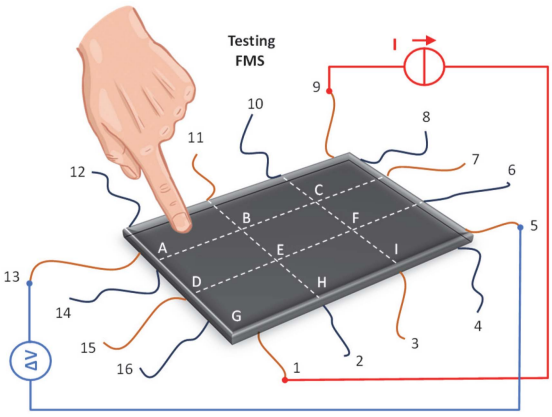

Fig. 6. Sketch represents the 9 FMS pressure zones and one of the 256 voltamperometric measures of the ERT procedure according to the "across" opposing injection scheme [11]. In the shown step, current I is applied across opposite electrodes 1 and 9, and one of the resulting voltage ΔV is measured across electrodes 5 and 13.

which can be attributed to the presence of a GNP network coating the pore walls of the foam [see Fig.1(e)]. Initially, when pressure is applied, the pores deform and the contacts between some adjacent GNPs break, resulting in decreased conductivity. As the pressure increases further, the unit cell collapses more, leading to the re-establishment of contacts between GNPs and enhancing overall conductance [6]. Notably, two maximum sensitivity values were observed: 0.13 kPa^{-1} at 3.9 kPa and 0.31 kPa^{-1} at 8.0 kPa. These findings suggest that the FMS will demonstrate a significant positive piezoresistive sensitivity within the pressure range 5–20 kPa (shaded region in Fig. 5) experienced during finger touch in our specific scenario.

B. Pressure Detection With ERT and ML Techniques

The acquired ERT data are used to employ a range of ML techniques (see Table 1) for the purpose of discerning pressure distribution on the surface of the FMS. By subdividing the foam surface into nine separate zones, labeled from A to I (see Fig. 6), the goal of the utilized classification algorithms was to precisely recognize the particular zones where deformation was induced either by the pressure of a single finger [single touch (ST)] or by the concurrent touch of two fingers at distinct points on different zones of the mat. In particular, in conducting the feasibility study for multitouch capabilities, we examined eight distinct double-touch (DT) configurations. To assess the effectiveness of ML methods, the standard metric of accuracy was used. Voltage data for algorithms' training were produced experimentally during the ERT process utilizing wooden cylinders with a diameter of 1 cm, upon which different weights were placed, specifically of 50, 100, 150, and 200 g. This setup aimed to replicate the pressure of a fingertip and simulate the application of various pressures on the surface of the FMS. During the implementation in MATLAB, we fine-tuned each model's hyperparameters using cross validation. We also preprocessed data and split them into training and testing sets to avoid overfitting. The

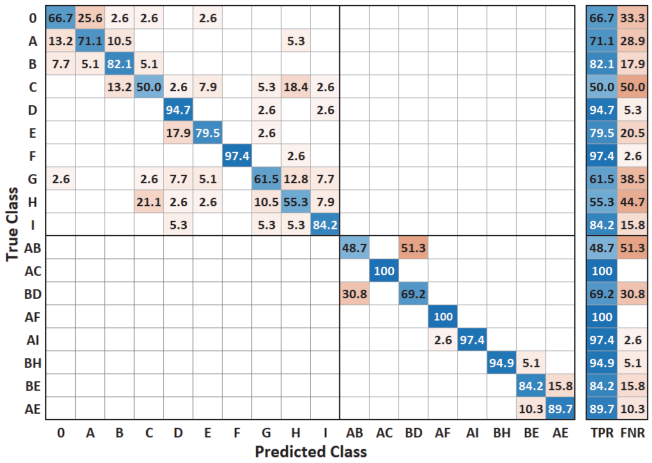

Fig. 7. Confusion matrix with TPR and FNR percentage values for each class. The class labeled 0 corresponds to the "no touch" scenario. Classes labeled with letters from A to I represent ST cases. Classes labeled with two letters indicate DT events, occurring in the corresponding zones of Fig. 6.

quadratic support vector machine (SVM) excelled for ST cases (when the ML algorithm is not trained for DT yet), accurately distinguishing distinct zones. The K-Nearest Neighbors (KNN) algorithm emerged as the top performer when also incorporating DT recognition. The confusion matrix of Fig. 7 shows the KNN classifier's performance in each class. The percentages along the diagonal represent the true positive rates (TPR), indicating the proportion of correctly classified observations for each true class (recall metric). The sum of the percentages along the columns, excluding the diagonal elements, represents the false negative rate (FNR), indicating the proportion of incorrectly classified observations for each true class.

It should be noted that when a touch occurs between two or more adjacent zones, the touch position could be estimated by considering the probability of belonging to each zone and utilizing triangulation techniques. All three algorithms—SVM, artificial neural network (ANN), and KNN—have the capability of providing probability values for this purpose. However, employing ANN might be more advantageous due to its direct estimation of probabilities.

IV. CONCLUSION

This research has the potential to contribute to various applications (e.g., SHM, soft robotics, and healthcare), offering new possibilities for precise and comprehensive touch detection, pressure monitoring, and deformation map recognition on large surfaces. Future developments will integrate ERT and ML techniques into sensor systems with larger mats to enable extensive pressure mapping, increasing resolution (i.e., using a denser grid), and improving multitouch detection capabilities as well as shape recognition. Currently, our objective is to integrate these solutions into beds or mattresses to enable continuous monitoring of the patient presence and sleeping position by recognizing pressure distribution between the body and the supporting surface.

ACKNOWLEDGMENT

This work was supported by co-funding from the European Union - Next Generation EU, within the context of The National Recovery and Resilience Plan, specifically under Investment Partenariato Esteso PE8 'Conseguenze e sfide dell'invecchiamento', as part of the 'Age-It' project (Ageing Well in an Ageing Society).

REFERENCES

[1] A. S. Fiorillo, C. D. Critello, and S. A. Pullano, "Theory, technology and applications of piezoresistive sensors: A review," *Sensors Actuators A, Phys.*, vol. 281, pp. 156–175, 2018.
[2] F. Sharif et al., "Synthesis of a high-temperature stable electrochemically exfoliated graphene," *Carbon*, vol. 157, pp. 681–692, 2020.
[3] X. Su et al., "A comparative study of polymer nanocomposites containing multi-walled carbon nanotubes and graphene nanoplatelets," *Nano Mater. Sci.*, vol. 4, no. 3, pp. 185–204, 2022.
[4] X. Dong, Y. Wei, S. Chen, Y. Lin, L. Liu, and J. Li, "A linear and large-range pressure sensor based on a graphene/silver nanowires nanobiocomposites network and hierarchical structural sponge," *Composites Sci. Technol.*, vol. 155, pp. 108–116, 2018.
[5] M. Jian et al., "Flexible and highly sensitive pressure sensors based on bionic hierarchical structures," *Adv. Funct. Mater.*, vol. 27, no. 9, 2017, Art. no. 1606066.
[6] M. Fortunato, I. Bellagamba, A. Tamburrano, and M. S. Sarto, "Flexible Ecoflex/graphene nanoplatelet foams for highly sensitive low-pressure sensors," *Sensors*, vol. 20, no. 16, 2020, Art. no. 4406.
[7] H. Kou et al., "Wireless wide-range pressure sensor based on graphene/PDMS sponge for tactile monitoring," *Sci. Rep.*, vol. 9, no. 1, pp. 1–7, 2019.
[8] E. Davoodi et al., "3D-printed ultra-robust surface-doped porous silicone sensors for wearable biomonitoring," *ACS Nano*, vol. 14, no. 2, pp. 1520–1532, 2020.
[9] P. N. Darma, M. R. Baidillah, M. W. Sifuna, and M. Takei, "Real-time dynamic imaging method for flexible boundary sensor in wearable electrical impedance tomography," *IEEE Sensors J.*, vol. 20, no. 16, pp. 9469–9479, Aug. 2020.
[10] D. Silvera-Tawil, D. Rye, M. Soleimani, and M. Velonaki, "Electrical impedance tomography for artificial sensitive robotic skin: A review," *IEEE Sensors J.*, vol. 15, no. 4, pp. 2001–2016, Apr. 2015.
[11] T. N. Tallman and D. J. Smyl, "Structural health and condition monitoring via electrical impedance tomography in self-sensing materials: A review," *Smart Mater. Struct.*, vol. 29, no. 12, 2020, Art. no. 123001.
[12] H. Chen, X. Yang, P. Wang, J. Geng, G. Ma, and X. Wang, "A large-area flexible tactile sensor for multi-touch and force detection using electrical impedance tomography," *IEEE Sensors J.*, vol. 22, no. 7, pp. 7119–7129, Apr. 2022.
[13] Y. Chen and H. Liu, "Location-dependent performance of large-area piezoresistive tactile sensors based on electrical impedance tomography," *IEEE Sensors J.*, vol. 21, no. 19, pp. 21622–21630, Oct. 2021.
[14] S. Quqa, Y. Shu, S. Li, and K. J. Loh, "Pressure mapping using nanocomposite-enhanced foam and machine learning," *Front. Mater.*, vol. 9, 2022, Art. no. 862796.
[15] H. Park, K. Park, S. Mo, and J. Kim, "Deep neural network based electrical impedance tomographic sensing methodology for large-area robotic tactile sensing," *IEEE Trans. Robot.*, vol. 37, no. 5, pp. 1570–1583, Oct. 2021.

Open Access funding provided by 'Università degli Studi di Roma "La Sapienza" 2' within the CRUI CARE Agreement